ОБЪЕДИНЕННЫЙ
ИНСТИТУТ
ЯДЕРНЫХ
ИССЛЕДОВАНИЙ
ДУБНА

E7 - 10675

B.Bochev, S.Iliev, R.Kalpakchieva,
S.A.Karamian, T.Kutsarova,
E.Nadjakov, Ts.Venkova

STUDY OF THE POPULATION AND DECAY OF HIGH-SPIN LEVELS IN ^{156}Er AND ^{160}Er USING THE REACTIONS ^{120,124}Sn(^{40}Ar,4n)

1977

E7 - 10675

B.Bochev, S.Iliev, R.Kalpakchieva,
S.A.Karamian, T.Kutsarova,
E.Nadjakov, Ts.Venkova

STUDY OF THE POPULATION AND DECAY OF HIGH-SPIN LEVELS IN ^{156}Er AND ^{160}Er USING THE REACTIONS ^{120,124}Sn(^{40}Ar,4n)

Submitted to "Nuclear Physics"

Бочев Б. и др.

E7 - 10675

Изучение процесса заселения и распада высокоспиновых уровней ^{156}Er, ^{160}Er в реакциях $^{120,124}Sn(^{40}Ar, 4n)$

Измерены интенсивности и времена заселения, а также времена жизни уровней полосы основного состояния (ПОС) изотопов $^{156,160}Er$. Использованы реакции $^{120,124}Sn(^{40}Ar,4n)^{156,160}Er$, применен допплеровский метод расстояния отдачи. Для изотопа ^{160}Er времена жизни уровней показывают такую же тенденцию слабого отклонения от модели жесткого ротатора, как и в известных случаях $_{70}Yb$, $_{72}Hf$; для ^{156}Er нельзя исключить заметное торможение переходов в области бэк-бендинга. Времена и интенсивности заселения ПОС измерены при двух энергиях для каждого изотопа. Обсуждается зависимость времен заселения ϕ_I от свойств изотопа и энергии бомбардирующих ионов. В простых предположениях сделан расчет среднего спина, уносимого γ-каскадом, времени протекания γ-каскада и сечения реакции $(^{40}Ar,4n)$.

Работа выполнена в Лаборатории ядерных реакций ОИЯИ.

Препринт Объединенного института ядерных исследований. Дубна 1977

Bochev B. et al.

E7 - 10675

Study of the Population and Decay of High-Spin Levels in ^{156}Er and ^{160}Er Using the Reactions $^{120,124}Sn(^{40}Ar,4n)$

The feeding intensities and times, as well as the lifetimes of the g.s.b. levels in the isotopes $^{156,160}Er$ have been measured. The measurements have been carried out in the reaction $^{120,124}Sn(^{40}Ar,4n)^{156,160}Er$ using the Doppler-shift recoil-distance method. For the isotope ^{160}Er, the level lifetimes show the same tendency of a small deviation from the rigid rotor model as in the known cases for $_{70}Yb$ and $_{72}Hf$, whereas in the case of ^{156}Er a considerable retardation of transitions seems to take place in the backbending region. The feeding times and intensities for the g.s.b. levels have been measured at two bombarding energies for each isotope. The dependence of the feeding times ϕ_I on the properties of the isotope and on the bombarding energy is discussed. The average spin carried off by the γ-ray cascade, the duration of the cascade and cross section for the reaction $(^{40}Ar,4n)$ have been calculated under simple assumptions.

Preprint of the Joint Institute for Nuclear Research. Dubna 1977

I. INTRODUCTION

In previous work [1,2], the feeding times and lifetimes for ground-state band (g.s.b.) levels in the doubly even isotopes ^{160,162,164,164}Yb and ^{166,168,170}Hf have been measured. The level lifetimes were found to differ slightly from the rigid-rotor model predictions: even in the backbending region, where $I=(12-16)\hbar$, transitions in the nuclei studied were retarded by a factor of less than 1.4 ± 0.2. In addition, the intensities and feeding times of rotational band levels were measured in the reaction (^{40}Ar, 4n). The level feeding time is generally equal to (1–15) ps in the spin range $(8-20)\hbar$ and varies with spin, and as one goes from one isotope to another. In the Hf isotopes, one has observed a second long-lived feeding component for the g.s.b. 6^+, 8^+ levels. In general, these results are in good agreement with the data obtained by other groups (see, e.g., refs. [3,4]). In ref. [5] the systematics of the feeding times and intensities for the g.s.b. levels in reactions of the type (HI, x n) have been presented. It has been concluded that it is appropriate to measure the feeding times as a function of both the bombarding energy and ion mass for a fixed reaction product with the purpose of obtaining information on the

possible dependence of the feeding times of the g.s.b. levels on the angular momentum of the compound nucleus.

In ref. /5/, it was noted that the mean value of the populated g.s.b. level spin, $\sqrt{\langle I^2 \rangle}$, varies slightly as the angular momentum of the compound nucleus, $\sqrt{\langle \ell^2 \rangle}$, increases. Therefore, with increasing ion mass (and increasing $\sqrt{\langle \ell^2 \rangle}$) a substantial increase in the number of the γ-rays emitted by the cascade preceding the population of the ground state band is expected. This agrees with the results of the measurements of the γ-ray multiplicities in the (HI,xn) reactions (see, e.g., refs. /6-9/). We have also noted earlier /5/ that the angular momentum distribution of the compound nucleus, at the stage following neutron evaporation, is limited from above and below and displaced rapidly towards higher spins with increasing ion energy. As a result, on the right-hand slope of the excitation function for the (HI,xn) reaction, the average spin of the nucleus, at the stage following neutron evaporation, may exceed $\sqrt{\langle \ell^2 \rangle}$ considerably, whereas it may be substantially smaller than $\sqrt{\langle \ell^2 \rangle}$ on the left-hand side. This is due to the separation of the nuclei according to their angular momenta, and to the division of the total distribution over ℓ into parts corresponding to the products of the evaporation of different numbers of neutrons. This regularity as it is has been confirmed by the recent measurements of the γ-ray multiplicities in the reactions $^{150}Nd(^{20}Ne,xn)$ /9/.

The purpose of the present work was to measure the feeding times for the g.s.b. levels in the deformed nucleus ^{160}Er and the transitional nucleus ^{156}Er, produced by the reactions ^{120,124}Sn(^{40}Ar,4n), as a function of the bombarding energy. It was intended to repeat the previous measurements of the life-times of the g.s.b. levels in these isotopes [4] with spins as high as possible. In addition to the verification of the considerations given in ref. [5] the task was to detect the possible substantial increase in the feeding time for the isotope $^{156}_{68}$Er$_{88}$, associated with the effects due to the second minimum in the total energy of the rotating nucleus at large deformations. This minimum was found in calculations [10] taking into account the shell correction using a macro-microscopic approach. According to this calculation, these effects are expected to manifest themselves most strongly in the case of nuclei with Z and N around 66 and 88, respectively.

II. EXPERIMENTAL PROCEDURE

Yrast levels in ^{156,160}Er were populated in the reaction (^{40}Ar,4n). The experiments were carried out using an external ^{40}Ar ion beam from the U-300 cyclotron with an energy varied in the range 140-200 MeV by Al degrader foils. The metallic targets, 1.8 mg/cm^2 thick, were made of the separated ^{120}Sn and ^{124}Sn isotopes. Use was made of the Doppler-shift recoil-distance method suggested and employed in previous work [4,11-13].

The experimental arrangement and data handling were described in refs.[1,2]. A high-precision Doppler chamber permitted measurement of the target-stopper distance to an accuracy of $\pm 2\mu m$ including the accuracy of the zero-distance measurement and deviations from the plane-parallel position of the target and stopper. This accuracy corresponds to a ± 0.3 ps accuracy of the time-of-flight measurement. The dependences $R_I(t)$, where R is the relative intensity of the Doppler-unshifted γ-line,

$$R_I = \left(\frac{N_u}{N_u + N_s}\right)_{I \to I-2}$$

(the s and u indices stand for Doppler-shifted and unshifted lines, respectively) were determined from the experimental γ-ray spectra measured at different target-stopper distances. The side feeding intensity of the g.s.b. levels,

$$P_I = (N_u + N_s)_{I \to I-2} - (N_u + N_s)_{I+2 \to I}$$

was determined experimentally in the units of the intensity of the $2^+ \to 0^+$ transition.

The experimental values of $R_I(t)$ were reproduced using a model[14], in which each g.s.b. level is populated via side feeding with an intensity P_I (measured experimentally) and the sought lifetime ϕ_I, as well as through the chain of sequential g.s.b. transitions with lifetimes τ_I. In some cases a two-component side feeding with lifetimes $(\phi_I)_1$ and $(\phi_I)_2$ was assumed. The problem was computed using the Gauss-Newton iteration procedure[15] with the purpose of finding the set of the parameters ϕ_I and τ_I. In order to check the stability of the results several

control solutions have been found assuming some parameters to be fixed.

Detailed measurements of a system of $R_I(t)$ values were done for the isotopes $^{156,160}Er$ at two projectile energies, 150 and 168 MeV. In addition, we measured the γ-line intensities as a function of energy in the range 145-200 MeV in order to estimate the shape of the excitation functions of the reactions.

III. RESULTS

Figs. 1 and 2 show the experimental values of $R_I(t)$ (dots) and the calculated decay curves of the levels for all the four sets of the $R_I(t)$ values measured. The lifetimes τ_I of the studied levels in the isotopes $^{156,160}Er$, and the calculated from τ_I values of $B(E2, I \to I-2)$, $B(E2, I \to I-2)/B_{rot}(E2, I \to I-2)$, quadrupole momentum $Q_0(I)$ and parameter $\beta(I)$ as functions of spin are presented in tables 1 and 2. The intensities of the transitions measured at two projectile energies, P_I, and the values of ϕ_I, are compared in tables 3 and 4. The lifetimes τ_I have been obtained from more detailed measurements at 150 MeV in ^{160}Er and at 168 MeV in ^{156}Er. The program computations for the second energy sets (168 MeV for ^{160}Er, and 150 MeV for ^{156}Er) were done with fixed values of τ_I found before.

IV. PROPERTIES OF YRAST LEVELS

The energies of the $I \to I-2$ transitions, listed in the tables, are taken from refs./4,16-18/. Some data on feeding in the reaction $^{152}Nd(^{18}O,4n)$ of not only the g.s.b.

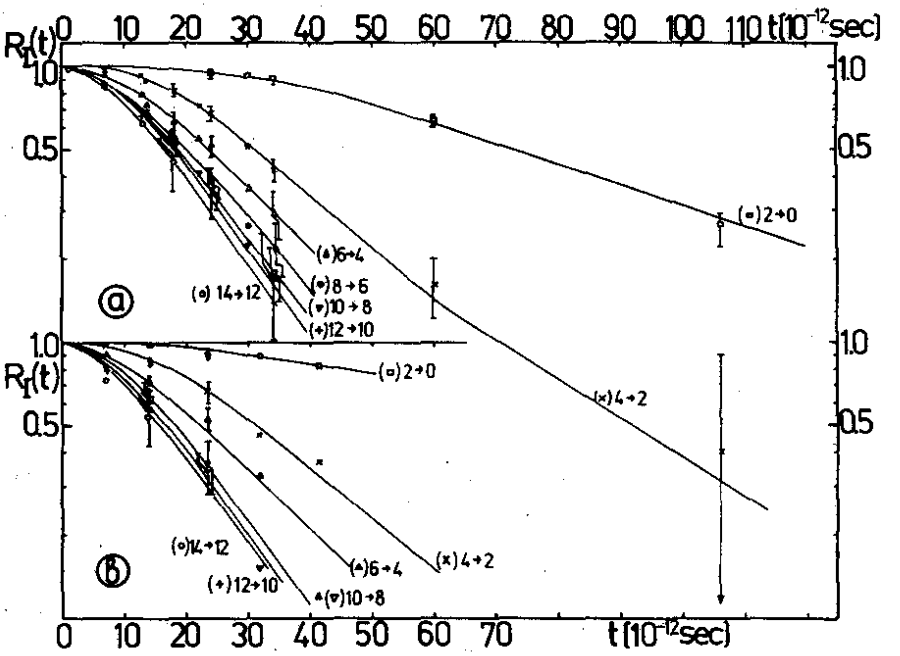

Fig. 1. Decay curves of the g.s.b. levels in ^{156}Er, measured at 168 MeV (a) and 150 MeV (b). Points are the experimental values of $R_I(t)$. Solid lines are the calculated best-fit curves. Spin I and the type of experimental point are indicated.

levels, but also the negative parity band 7^-, 9^-, 11^-,... and the positive parity band with odd spins 9^+, 11^+, 13^+ in ^{156}Er are presented in ref. /18/. The level scheme for ^{156}Er from ref. /18/ is shown in fig. 3. In

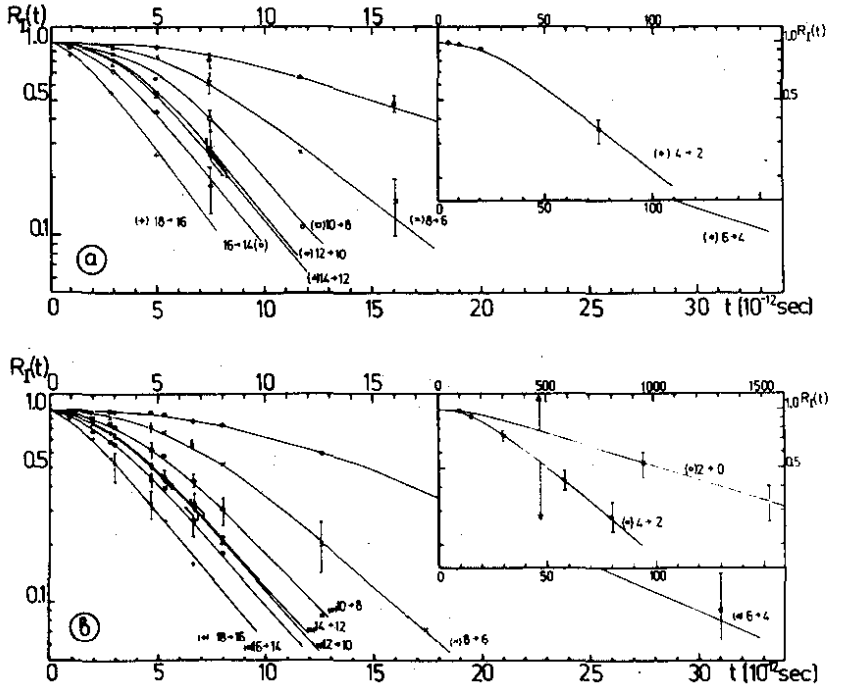

Fig. 2. The same as in Fig. 1, for ^{160}Er.

the measured spectra, we also observed the 460, 433, 290 and 531 keV lines corresponding to the transitions $9^- \rightarrow 7^-$, $11^- \rightarrow 9^-$, $11^- \rightarrow 10^+$, $9^- \rightarrow 8^+$, and the 414, 481 and 531 keV lines corresponding to the transitions $11^+ \rightarrow 9^+$, $13^+ \rightarrow 11^+$, $9^+ \rightarrow 8^+$. The experimental fact that the side feeding of the 6^+, 8^+, and 10^+ levels has a considerable intensity (see table 3) is in agreement with the level scheme (fig. 3). However, the high intensity of some of the transitions mentioned contradicts the quan-

Table 1

The lifetimes τ_I of the g.s.b. levels in the isotope ^{156}Er, determined experimentally and the values of $(B(E2, I \to I-2)$, Q_0 , β and the ratio of the lifetime to the values obtained in the rigid rotor model, $\tau_I / \tau_{I\,rot}$, derived from the τ_I values

Spin(ħ) I → I−2	Energy (KeV)	Lifetime (pcsec)	B(E2) $_{exp.}$ $[e^2b^2]$	Q_0 (barn)	β	Lifetime exp/rot
2 → 0	344.2	50.05 ± 1.81	0.322 ± 0.012	4.020 ± 0.073	0.182 ± 0.003	1.000*)
4 → 2	452.7	7.25 ± 0.73	0.576 ± 0.058	4.50 ± 0.22	0.203 ± 0.010	0.80 ± 0.08
6 → 4	543.3	2.93 ± 0.45	0.578 ± 0.087	4.30 ± 0.32	0.194 ± 0.015	0.88 ± 0.13
8 → 6	618.5	2.35 ± 0.85	0.378 ± 0.110	3.40 ± 0.51	0.154 ± 0.023	1.40 ± 0.42
10 → 8	674.4	2.25 ± 1.00	0.257 ± 0.128	2.76 ± 0.69	0.126 ± 0.031	2.12 ± 1.06
12 → 10	682.1	4.26 ± 2.60	0.128 ± 0.077	1.93 ± 0.58	0.089 ± 0.027	4.32 ± 2.59
14 → 12	522.7	8.1 ± 4.8	0.253 ± 0.154	2.70 ± 0.81	0.123 ± 0.037	2.21 ± 1.33

*) normalization to experiment; the energy values are taken from refs. [16,18].

titative balance of intensities on the condition of the conservation of the total intensity in the decay scheme (fig. 3). This permits the assumption that these lines due

Table 2

The same as in Table 1, for ^{160}Er

Spin(ħ) I→I-2	Energy (KeV)	Lifetime (pcsec)	B(E2) exper'm (e^2b^2)	Q_o (barn)	β	Lifetime exp/rot
2→0	125.6	1326 ± 45	0.851 ± 0.029	6.54 ± 0.11	0.286± 0.005	1.000*)
4→2	263.8	46.67± 1.52	1.236± 0.040	6.59 ± 0.11	0.289± 0.005	0.984 ± 0.032
6→4	375.3	7.78 ± 0.41	1.354 ± 0.072	6.58 ± 0.17	0.288 ± 0.008	0.989 ± 0.052
8→6	463.7	2.44 ± 0.61	1.521 ± 0.381	6.81 ± 0.85	0.298± 0.037	0.922 ± 0.231
10→8	531.7	1.26 ± 0.31	1.50 ± 0.37	6.67 ± 0.84	0.292 ± 0.036	0.961 ± 0.242
12→10	579.2	0.84 ± 0.21	1.47 ± 0.37	6.54 ± 0.82	0.286 ± 0.035	0.999 ± 0.249
14→12	592.2	0.90 ± 0.22	1.23 ± 0.30	5.96 ± 0.75	0.262 ± 0.033	1.210 ± 0.312
16→14	533.9	1.57 ± 0.20	1.17 ± 0.15	5.80 ± 0.36	0.255 ± 0.016	1.27 ± 0.16
18→16	556.1	0.98 ± 0.28	1.54 ± 0.45	6.62 ± 0.96	0.289 ± 0.042	0.977 ± 0.284

to ^{156}Er interfere with the lines of 532 keV ($21/2^+ \rightarrow 17/2^+$) and 414.8 keV ($21/2^+ \rightarrow 17/2^+$) in ^{155}Er and ^{157}Er, respectively (the transition energies of $^{155,157}Er$ are taken from ref.[20]). This assumption does not contradict the probable cross sections for the evaporation of three or five neutrons, since the excitation functions for the given compound nucleus are wide enough to overlap over a considerable energy interval. The decay curves for the 433, 531, 481 and 414 keV lines have been

Table 3

The optimal set of parameters: feeding times ϕ_I and lifetimes τ_I, obtained by reproducing the experimental decay curves $R_I(t)$ for the isotope ^{156}Er at two bombarding energies. P_I are the experimental values of side feeding intensities.

I(ħ)	τ_I [pcsec]	E_L=150 MeV		E_L=168 MeV	
		ϕ_I[pcsec]	P_I(%)	ϕ_I[pcsec]	P_I(%)
2	50.05± 1.81	–	0	–	0
4	7.25± 0.73	65 ± 39	10 ± 2	–	0
6	2.93± 0.45	15 ± 9	15 ± 2	91 ±54 31 ±18	4 ±1 6 ±2
8	2.35± 0.85	29 ±21	35 ± 4	22 ±15	36±4
10	2.25± 1.00	17 ± 12	10 ± 2	17 ±13	15±2
12	4.26 ± 2.60	8 ± 6	8 ± 2	10 ±7	10±2
14	8.1 ± 4.8	11 ± 5	22± 4	11 ±7	25±4

measured and the times of their decay to the e^{-1} level of the total intensity, θ, were obtained to be 24.5, 26.0, 18.0 and 24.0 ps, respectively. However, due to the difficulties involved in the unambiguous identification of the transitions, these decay curves have not been presented or included in the g.s.b. data analysis. In the case of ^{160}Er,

Table 4

The same as in Table 3, for the isotope ^{160}Er

I(ħ)	τ_I (psec)	E_L=150 MeV		E_L=168 MeV	
		τ_I(psec)	P_I(%)	τ_I(psec)	P_I(%)
2	1326± 45	–	0	–	0
4	46.67± 1.52	–	0	–	0
6	7.78 ± 0.41	4.52 ± 2.10	8 ± 2	4.53 ± 0.44	11 ±2
8	2.44± 0.61	6.74 ± 6.72	12±3	5.58 ± 0.44	14 ± 3
10	1.26 ± 0.31	5.12 ± 2.82	20±3	6.94 ± 0.43	25± 4
12	0.84 ± 0.21	3.39 ± 2.02	27±4	3.01 ± 0.43	13 ± 2
14	0.90 ± 0.22	2.93 ± 2.22	5± 1	4.76 ± 0.44	7 ± 1
16	1.57 ± 0.20	0.61 ± 0.53	5± 1	0.50 ± 0.42	4 ± 1
18	0.98 ± 0.28	3.10 ± 1.30	23±3	2.86 ± 1.10	26± 3

an overlap of the 463.7 keV $8^+ \rightarrow 6^+$ and 556.1 keV $18^+ \rightarrow 16^+$ transitions with the lines attributed to ^{159}Er, the 464.5 keV $(25/2^+ \rightarrow 21/2^+)$ and 556.0 keV $(29/2^+ \rightarrow 25/2^+)$ ones, is possible. Although the transition intensities were corrected by interpolating the intensity of the adjacent transitions, the decay curves may be somehow distorted in these cases.

The values of $B(E2, I \rightarrow I-2)$, $Q(I \rightarrow I-2)$, $\beta(I \rightarrow I-2)$, and r/r_{rot} for the isotope ^{156}Er are presented in table 1. For I=2,4,6 the τ_I values

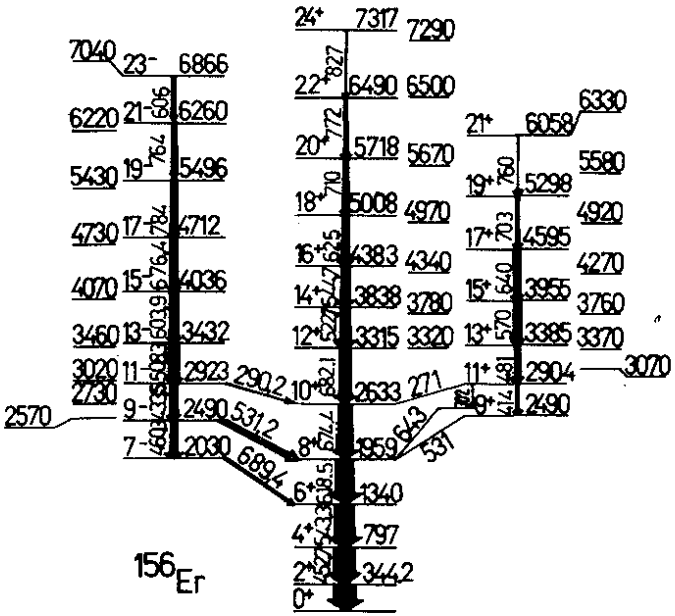

Fig. 3. The level scheme for ^{156}Er, taken from ref./18/. Both the experimental /18/ and calculated values/19/ of the level energy are presented.

agree with the results of ref./4/ within experimental accuracies. For higher spins, one can see that the automatic fitting of parameters leads to a solution (with a minimum value of χ^2), in which the lifetimes of the levels 10^+, 12^+ and 14^+ exceed the rigid rotor values by a factor of (2-4) to a 50% accuracy. Despite the considerable inaccuracy, this result appears to be substantially different from that obtained in the backbending region for the ytterbium and hafnium

isotopes[1,2]. At the same time, the authors of ref.[21] observed a considerable (by a factor of 10 and 25) retardation of the $8^+ \to 6^+$ and $10^+ \to 8^+$ transitions in the isotope ^{134}Ce, which, like ^{156}Er, is a transitional nucleus between deformed and spherical ones. Therefore, it is likely that the value of the retardation factor for transitions in the backbending region depends on the details of the structure of the nucleus. To check the stability of the result obtained for ^{156}Er (tables 1 and 3), a calculation has been carried out involving the values of the lifetimes of the 12^+ and 10^+ levels fixed to be $1.37\tau_{rot}$ and $1.38\tau_{rot}$ according to the results for Yb and Hf. The other parameters were sought to provide the best reproduction of the data. By varying the parameters ϕ_I one has obtained a solution characterized by the quantity χ^2 exceeding inconsiderably these obtained in the first version of calculation (tables 1 and 3). The parameters τ_I for $I \neq 10,12$ do not differ, within the error, from those obtained in the first calculation. Nevertheless, the solution given in tables 1 and 3 is favoured not only by the minimum χ^2 value, but also by the fact that in this case the ϕ_I values increase by a factor of 2-2.5 as one goes from the $14^+, 12^+$ levels to the 10^+, 8^+, 6^+ levels, i.e., in the spin region where, as fig. 3 shows, the g.s.b. is fed by two other bands. No such a change has been observed in the case of the solution involving the τ_{10} and τ_{12} values fixed to be close to τ_{rot}. It is noteworthy that the values of ϕ_{10} and ϕ_{12} (table 3) do not contradict the times θ measured experimentally for the 433, 460, 531 and 414 keV lines (see above). These

arguments confirm indirectly the validity of the first version of the solution with $\frac{\tau_{10}}{\tau_{rot}} = 2.12 \pm 1.06$, $\frac{\tau_{12}}{\tau_{rot}} = 4.32 \pm 2.59$, $\frac{\tau_{14}}{\tau_{rot}} = 2.21 \pm 1.53$. For a second check of the solution, a calculation was made assuming two time components of level feeding. For the 6^+ level alone, one has found a substantially different lifetime of the second component, $\phi_6' \approx 90$ ps, its intensity being $4 \pm 1\%$.

The results on ^{160}Er are listed in tables 2 and 4. Here, the situation is simpler than for ^{156}Er. The retardation factor for the $16^+ \to 14^+$ and $14^+ \to 12^+$ transitions is about 1.2-1.3, which is in agreement with the values measured for ^{158}Er /3/, ^{164,166}Yb /1/ and ^{168}Hf /2/. The values of lifetimes τ_I and, consequently, B(E2), quadrupole momentum Q_0 and deformation parameter β for levels in ^{160}Er with spins (2–8)$\hbar$ coincide, within the accuracy, with those found in ref. /4/.

V. FEEDING INTENSITIES OF YRAST STATES

The feeding intensities of the g.s.b. levels in the isotopes ^{156}Er and ^{160}Er at two energies of ^{40}Ar ions are presented in tables 3 and 4, and in fig. 4. One can see that the feeding functions for the g.s.b. levels in ^{156}Er and ^{160}Er differ, but vary inconsiderably with projectile energy. Table 5 gives the mean squares of spins of the level populated, $\sqrt{\langle I^2 \rangle}$.

Besides the values of $\sqrt{\langle I^2 \rangle}$, table 5 shows the values of the maximum angular momentum of the compound nucleus, ℓ_{max}, calculated within the framework of the sharp cut-off

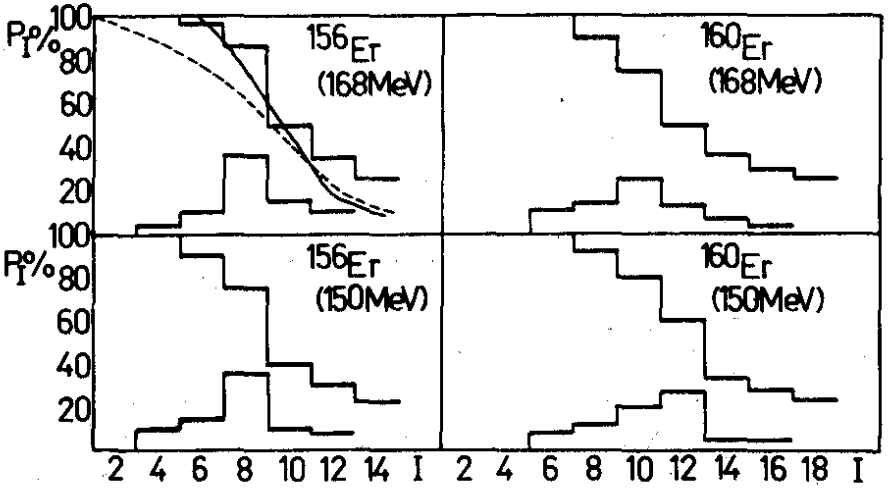

Fig. 4. The feeding intensity of the g.s.b. levels for the isotopes ^{156,160}Er in the reactions ^{120,124}Sn(^{40}Ar,4n) at two bombarding energies. The integral and differential intensities of each level are shown by histograms. Solid and dashed lines show the data for the reactions ^{160}Dy(^{4}He,8n)^{156}Er (108 MeV) and ^{144}Nd(^{16}O,4n)^{156}Er (100 MeV) from ref. /17/.

approximation at r_0 = 1.47 fm, which does not contradict the experimental estimate of the excitation function for the reaction ^{120}Sn(^{40}Ar,4n) (see the following). The value of the critical angular momentum ℓ_{crit} for the nuclear fusion reaction, first introduced in refs. /22,23/, was calculated using a formula taken from ref. /5/. This formula was deduced assuming the balance between the centrifugal and contracting forces

Table 5

The values of the angular momenta characterizing the reactions $^{120,\ 124}$Sn(^{40}Ar,4n) (notation is given in the text).

	E_L MeV	E_c MeV	l_{max}	l_{crit}	l_l	l_h	$\sqrt{\frac{l_l^2+l_h^2}{2}}$	$\sqrt{\langle I^2\rangle}$
^{120}Sn(^{40}Ar,4n)	150.0	112.5	36.3	72	0	20	14.2	10.3
	168.5	126.4	64.3	72	26.4	44.7	36.0	11.0
	189.0	141.7	85.0	72	49.5	60.7	55.2	11.5
^{124}Sn(^{40}Ar,4n)	150.0	113.1	43.4	73	0	30.8	21.5	13.8
	168.5	127.1	66.8	73	37.8	51.0	44.6	13.9

acting in two touching nuclei. The considerations on ℓ_{crit} given in ref.[5] are similar to those presented earlier [24].

The angular momentum distributions of compound nuclei, at the stage following neutron evaporation, for a fixed final product of the reaction (HI, x n) were first calculated for some specific cases in ref.[25] using a statistical approach and numerical methods. Qualitative considerations on these distributions were put forward in ref.[26]. In ref.[5], we proposed a simple graphical way of finding the angular momentum distribution of com-

pound nuclei after neutron evaporation for a fixed reaction product under the following simplifying assumptions:

(i) Each neutron evaporated carries off a strictly definite amount of thermal excitation energy, $B_{ni}+2T$, but not any angular momentum;

(ii) The probability of the evaporation of the $(i+1)$th neutron is equal to unity if the thermal excitation energy of the neutron emitting nucleus, $(E_i^* - E_{rot}) > 3/2\,B_{n,i+1}$, and this probability is equal to 0 if $(E_i^* - E_{rot}) \leq 3/2\,B_{n,i+1}$. Similarly to ref./5/ in these approximations we obtain the values of ℓ_ℓ and ℓ_h, i.e., the lower and upper limits of the angular momentum distribution of compound nuclei for a fixed product of the evaporation of x neutrons

$$(\ell_\ell)^2 = \frac{2J}{\hbar^2}\left(E^* - \sum_{i=1}^{x+1} B_{ni} - 0.5\,B_{n,x+2} - 2(x+1)T - \Delta\right), \qquad (1)$$

$$(\ell_h)^2 = \frac{2J}{\hbar^2}\left(E^* - \sum_{i=1}^{x} B_{ni} - 0.5\,B_{n,x+1} - 2xT - \Delta\right). \qquad (2)$$

Here the yrast line is calculated in a parabolic approximation, $E_{rot} = \frac{\hbar^2}{2J}\,\ell^2 + \Delta$. Eqs. (1) and (2) permit also calculation of the excitation function curve σ_{xn} for the reaction (HI, xn). Fig. 5 shows the dependence of ℓ^2_{max} on E_c of ions taking into account ℓ^2_{crit} for the reaction $^{120}Sn(^{40}Ar,4n)^{156}Er$, as well as the straight lines ℓ^2_ℓ and ℓ^2_h for the same reaction. Vertical intercepts in fig. 5 define the cross sections for the reaction (HI, xn) at different ion energies:

$$\sigma_{xn} = \frac{\pi(\ell_h^2 - \ell_\ell^2)}{2(0.155)^2\,\frac{A_1 A_2}{A_1 + A_2}\,E_c}, \qquad (3)$$

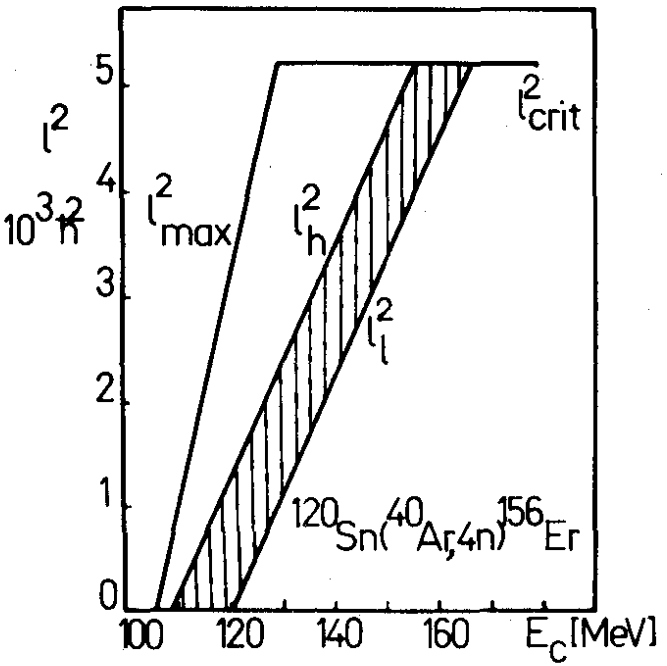

Fig. 5. The dependence of the values of ℓ^2_{max} and ℓ^2_{crit} on energy E_c (in the c.m.s.) for the reaction involving the compound nucleus formation in the system $^{120}Sn + ^{40}Ar$. The angular momentum region limited by the straight lines ℓ^2_ℓ and ℓ^2_h is for the product of the evaporation of four neutrons.

where ℓ_h and ℓ_ℓ are expressed in the $\hbar$ units, E_c is in MeV, and σ_{xn} is in fm^2. The so-calculated excitation function for the reaction $^{120}Sn(^{40}Ar,4n)^{156}Er$ and normalized experimental data (points) are shown in fig.6. The parameter $\hbar^2/2J$ was taken to be equal to 8.68 keV in agreement with the moment

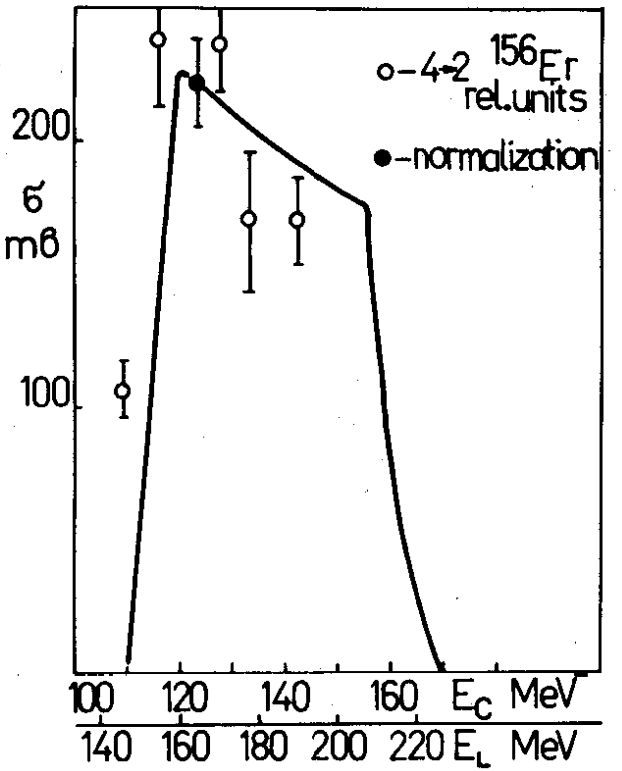

Fig. 6. The calculated excitation function for the reaction $^{120}Sn(^{40}Ar,4n)^{156}Er$ (solid curve). The points show the normalized experimental values.

of inertia for ^{156}Er, determined from the energy of the g.s.b. $16^+ \to 14^+$ transition in the backbending region. One should note that this calculation is similar to that described in ref.[5] made to find the angular momentum distribution of compound nuclei after neutron evaporation. The results of calculating the excitation function for the reaction

$^{118}Sn(^{40}Ar,5n)$ are presented in ref.[27]. This calculation seems to be made under similar assumptions and leads to an excitation function of similar shape. However, the lower limit of the angular distribution, mentioned in ref.[5] and in the present paper, is due to the fixation of the final product (nuclei with $\ell < \ell_\varphi$ pass into the channel of the evaporation of a large number of neutrons) and has nothing to do with the lower limit of the angular momentum of the entrance channel for ^{84}Kr ions, observed in ref.[27]. The excitation functions for other reactions (HI,xn) can be calculated using eqs. (1)-(3); but such a calculation is invalid for compound nuclei having considerable cross sections for fission[28] or evaporation of charged particles, which leads to a distortion of the angular momentum distribution of nuclei in neutron evaporation channels. For medium-weight compound nuclei, the positions of the lines in a plot similar to that of fig. 5 may vary considerably as a function of ion mass (which determines the slope of the straight line ℓ^2_{max} in fig. 5), and of neutron number and energy release (which determine the horizontal displacement of the pair of the straight lines ℓ^2_ℓ and $\ell^2_\hbar$). Some possibilities are shown in fig. 7. One can see that the angular momentum distribution for a fixed x may be restricted by different limits depending on bombarding energy, i.e., eq. (3) should be rewritten in the following form

$$\sigma_{xn} = \frac{\pi(\ell_2^2 - \ell_1^2)}{2(0.155)^2 \frac{A_1 A_2}{A_1 + A_2} E_c}, \qquad (4)$$

where

$$\ell_1 = \begin{cases} 0 \\ \ell_\ell \end{cases} \qquad \ell_2 = \begin{cases} 0 \\ \ell_{max} \\ \ell_h \\ \ell_{crit} \end{cases}$$

Now we return to table 5, which gives the values of ℓ_ℓ and ℓ_h for three energies of the ^{40}Ar ions in the case of ^{156}Er and for two projectile energies in the case of ^{160}Er, as well as the mean values of the angular momentum of the reaction product at the stage following neutron evaporation, $\sqrt{\frac{\ell_h^2 + \ell_\ell^2}{2}}$. Thus, we know the average spin values at the beginning of the γ-ray cascade, $\sqrt{\frac{\ell_h^2 + \ell_\ell^2}{2}}$, and those for the g.s.b. level populated, $\sqrt{\langle I^2 \rangle}$. The difference between these spins is carried off by the γ-ray cascade whose duration is known from tables 3 and 4, and figs. 1 and 2. From table 5 it is seen that $\sqrt{\frac{\ell_h^2 + \ell_\ell^2}{2}}$ increases very rapidly with ion energy. This allows one to say that the measurements of the ϕ_I values at two ion energies check the dependence of ϕ_I on the widely varying angular momentum carried off by the γ-ray cascade preceding the g.s.b. transition: $\sqrt{\frac{\ell_h^2 + \ell_\ell^2}{2}} - \sqrt{\langle I^2 \rangle}$.

VI. FEEDING TIMES OF YRAST STATES

Tables 3 and 4 present the side feeding times ϕ_I of the g.s.b. states, which were

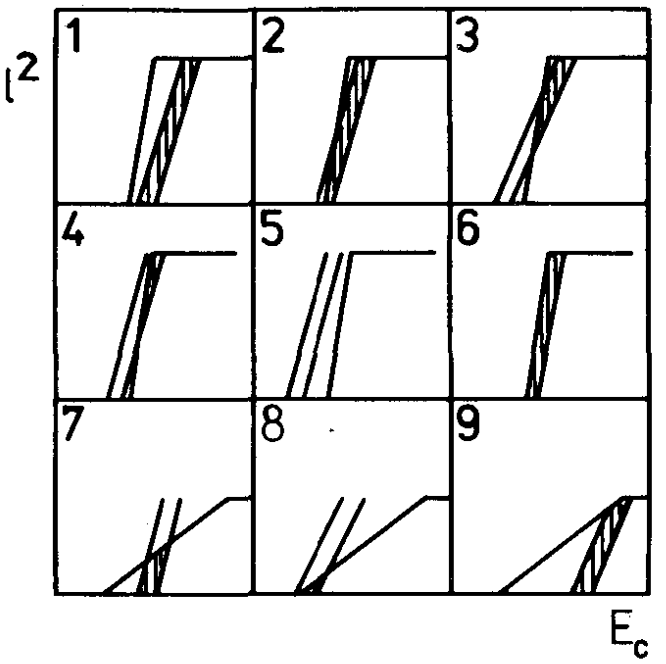

Fig. 7. Possible positions of the lines similar to those shown in fig. 5, which determine the shape of excitation functions for the reactions (HI, xn).

measured at two ^{40}Ar ion energies for the isotopes ^{156}Er and ^{160}Er. The ϕ_I values do not include the time of feeding via g.s.b. transitions (except ϕ_{I_m}, where I_m is the maximum spin of the g.s.b. levels observed). The θ_I values determined directly from the decay curves $R_I(t)$ (figs. 1,2) as the interval of time required for the function $R_I(t)$ to decrease by a factor of e ($R_I(\theta_I) = e^{-1}$) are

given in table 6. Therefore, the θ_I values include both the g.s.b. feeding and side feeding times with corresponding weight factors.

Table 6

Total feeding and decay time (ps) θ_I, of the levels (see the text) determined experimentally for ^{156}Er and ^{160}Er at two bombarding energies, compared with the values of $T_f(I)$ calculated using eq. (5) for the same reactions. $T_f(I) \equiv \tau_f$

Isotope	E_L (MeV)	I(ħ)	18	16	14	12	10	8	6	4
^{156}Er	150	θ_I			20.5±0.7	21.5±0.5	22.9±0.5	≈26	28±0.7	38.5±0.7
		τ_f			5.9	12.3	26.7			
	168	θ_I			20.7±0.5	22.5±0.5	23.4±0.5	25.3±0.5	29.4±0.7	38.0±0.7
		τ_f			7.5	13.9	28.3			
^{160}Er	150	θ_I	4.2±0.7	5.4±0.7	6.0±0.5	5.9±0.5	7.1±0.5	9.8±0.5	17.6±0.7	64.2±1.0
		τ_f		1.6	3.5	7.4	16.1			
	168	θ_I	4.0±0.7	5.3±0.7	6.2±0.5	6.4±0.5	7.9±0.5	10.3±0.5	18.1±0.7	64.7±1.0
		τ_f		2.7	4.6	8.5	17.2			

The data presented in tables 3, 4 and 6 permit the following conclusions:

(i) The values of ϕ_I and θ_I measured for a given isotope at two ion energies differ slightly in spite of a strong increase with energy in the angular momentum carried away

by the γ-ray cascade preceding the ground state band, and (ii) the values of ϕ_I and θ_I for ^{156}Er exceed considerably (by a factor of about 4) those for ^{160}Er, and this is in qualitative agreement with the predictions of ref.[10]. In addition, the θ_I values for ^{156}Er at I=6,4 are somewhat larger than those obtained experimentally earlier[4]. In ref.[29] the feeding time for the g.s.b. 8^+ level in ^{158}Yb which, like ^{156}Er, is also a transitional nucleus, was obtained to exceed 20 ps, i.e., close to our results for ^{156}Er.

The feeding time calculation may be made under the following assumptions: first, the cascade preceding the g.s.b. involves sequential E2 transitions described by the rotational law for the level energy as $E_I = \hbar^2/2J\ I(I+1)$, at $\hbar^2/2J = \text{const}$; second, the cascade starts at spin $I_{max} = \sqrt{\frac{\ell_h^2 + \ell_\ell^2}{2}}$ and ends at $I_{min} = \sqrt{\langle I^2 \rangle}$, and, third, the cascade is delayed for a negligible time. Under these assumptions the T_f value comparable with the experimental θ values has been obtained, i.e.,

$$\theta \sim T_f = \frac{0{,}271}{(1+\alpha) Q_0^2 (\hbar^2/2J)^5} \sum_{\substack{I = I_{min} \\ (I\text{-even})}}^{I_{max}-2} \frac{2I+5}{(4I+6)^4 (I+1)(I+2)}, \quad (5)$$

where θ and T_f are expressed in ps, Q_0 is in barns, $\hbar^2/2J$ is in MeV, and I is in the $\hbar$ units. The summation is made over the even values of I. If the summation limit I_{min} or $I_{max}-2$ has a value lying between two even numbers, the boundary term of the sum is substituted by a linear combination of the summed function at two even values of I close

to I_{min} or $(I_{max}-2)$ with the corresponding weight factors.

In eq. (5) the numerical values of parameters were taken as follows: $\alpha = 0$, $Q_0 = 4.02$ b, $\hbar^2/2J = 8.68 \times 10^{-3}$ MeV for ^{156}Er, and $\alpha = 0$, $Q_0 = 6.54$ b, $\hbar^2/2J = 7.93 \times 10^{-3}$ MeV for ^{160}Er. The Q_0 values (for the $2^+ \to 0^+$ transitions) are taken from tables 1 and 2, the $\hbar^2/2J$ values are calculated from the energy of the $16^+ \to 14^+$ transition for ^{156}Er /18/ and from the energy of the $18^+ \to 16^+$ transition for ^{160}Er. /16/ The following values were obtained: $T_f = 26.9$ ps ($E_L = 150$ MeV), $T_f = 21.1$ ps ($E_L = 168$ MeV) for ^{156}Er, and $T_f = 3.9$ ps ($E_L = 150$ MeV), $T_f = 4.9$ ps ($E_L = 168$ MeV) for ^{160}Er. The value of $\sqrt{\frac{\ell_p^2 + \ell_h^2}{2}}$ for ^{156}Er at 150 MeV, presented in table 5, is equal to $14.1\hbar$, which seems to be an underestimated value. Therefore, in the calculation using eq. (5) I_{max} was taken to be $20\hbar$, i.e., close to that for ^{160}Er at the same energy.

Since the summed series of eq. (5) decreases rapidly with spin, the largest contribution to the sum comes from terms with I close to I_{min}. It is clear that this calculation may involve a considerable error due to the deviations of the γ-ray energies from the rotational law with $\hbar^2/2J = \text{const}$ for the g.s.b. transitions below the backbending region, as well as for the transitions along other bands, and interband transitions. A change in the multipolarity is still more important for interband transitions. Another inaccuracy of the calculation using eq. (5) is due to that the thermal excitation energy left after the evaporation of x neutrons, $E^*_{xn} - E_{rot}(I_{max})$, was not taken into account.

This energy may either increase the average energy of the transitions, conserving the number of transitions, i.e., decrease T_f, or lead to additional (possibly dipole) γ-transitions carrying away the thermal energy with small changes in the angular momentum, i.e., increase T_f.

Now we shall discuss the T_f values obtained for ^{156}Er and ^{160}Er. The increase in T_f for ^{156}Er in going from 168 MeV to 150 MeV is associated with a decrease in $\sqrt{\langle I^2 \rangle}$. Transitions with spins $I \geq 20\hbar$ make a small contribution to T_f, resulting in a 1 ps increase in T_f as one goes from 150 MeV to 168 MeV and as I_{max} increases from $21.5\hbar$ to $44.6\hbar$ (in the case of ^{160}Er). The difference between the calculated values of T_f for the two isotopes is mainly due to different values of $I_{min} = \sqrt{\langle I^2 \rangle}$ (see table 5) and different Q_0 and $\hbar^2/2J$ values.

Thus, despite the rough approximations of the calculation, its result agrees with the experimental values of θ for spins close to $\sqrt{\langle I^2 \rangle}$ for each isotope. A detailed comparison of the θ_I values with the calculated values of $T_f(I)$ is given in table 6. The T_f values for $I \leq 8\hbar$ are not presented because the moments of inertia and, consequently, the transition energies of nuclei with such spins are considerably different from those assumed in the calculation for $\hbar^2/2J = \text{const}$. In addition, for ^{156}Er at $I \leq 10\hbar$, interband transitions having an irregular dependence of the energy on spin I play an important part. Although for $I = 12, 14\hbar$ in ^{156}Er the T_f values become smaller than θ_I, they are comparable with ϕ_I (see

table 3). This seems to be due to the fact that in calculating T_f we did not take into account the observed retardation factors of the $14^+ \to 12^+$ and $12^+ \to 10^+$ g.s.b. transitions, equal to 4 and 2, respectively (see table 1).

The experimental results allow one to conclude that the difference in the θ_I values for each isotope, associated with the projectile energy, does not exceed 1-2 ps and agrees with the calculation.

For ^{160}Er, agreement between T_f and θ_I is somewhat better than for ^{156}Er. In the latter case, the T_f values (see table 6) display the I dependence similar to that of ϕ_I (see table 3).

Thus, the experimentally observed independence (within 1-2 ps) of the feeding times on the projectile energy (despite the fact that with increasing ion energy the spin carried away by the γ-ray cascade increases considerably) and an increase in the feeding time as one goes from ^{160}Er to ^{156}Er are reproduced fairly well by the calculation using eq. (5) under simple assumptions.

The authors are thankful to Professors G.N.Flerov and Yu.Ts.Oganessian for their interest in and support of the work. Thanks are also due to N.Djarov and V.G.Subbotin for participating in making the experimental equipment, and the U-300 staff for providing good operation of the accelerator.

REFERENCES

1. Bochev B. et al. Nucl.Phys., 1976, A267, p. 344; JINR, E7-9626, Dubna, 1976.
2. Bochev B. et al. Nucl.Phys., 1977, A282, p.159. JINR, E7-10180, Dubna, 1976.

3. Ward D. et al. Phys.Rev.Lett., 1973, 30, p.493; Ward D. et al. Izv. Akad.Nauk SSSR (ser. fiz.), 1975, 39, p.37.
4. Diamond R.M. et al. Phys.Rev.Lett., 1969, 22, p.546; Newton J.O., Stephens F.S., Diamond R.M. Nucl.Phys., 1973, A210, p.19.
5. Bochev B. et al. Yad. Fiz., 1976, 23, p.520; JINR, P7-8676, Dubna, 1975.
6. Tjøm P.O. et al. Phys.Rev.Lett., 1974, 33, p.593; Banaschik M.V. et al. Phys. Rev.Lett., 1975, 34, p.892; Simon R.S. et al. Phys.Rev.Lett., 1976, 36, p.359.
7. Der Mateosian E., Kistner O.C., Sunyar A.W. Phys.Rev.Lett., 1974, 33, p. p.596.
8. Hagemann G.B. et al. Nucl.Phys., 1975, A245, p.166; Halbert M.L. et al. Nucl. Phys., 1976, A259, p.496.
9. Sarantites D.G. et al. Phys.Rev., 1976, C14, p.2138.
10. Neergård K., Pashkevich V.V. Phys.Lett., 1975, 59B, p.218; JINR, P4-8947, Dubna, 1975; Neergård K., Pashkevich V.V., Frauendorf S. Nucl.Phys., 1976, A262, p.61; JINR, P4-9194, P4-9195, P4-9196, Dubna, 1976.
11. Alexander T.K., Allen K.W. Can.J.Phys., 1965, 43, p.1563.
12. Jones K.W. et al. Phys.Rev., 1969, 178, p.1773.
13. Bochev B. et al. Phys.Scripta, 1973, 6, p.243; JINR, E7-6721, Dubna, 1972; Bochev B. et al. Yad.Fiz., 1972, 16, p.633; JINR, P7-6415, Dubna, 1972.
14. Bochev B., Alexandrov L., Kutsarova T. JINR, P5-7881, P5-8321, Dubna, 1974.
15. Alexandrov L. JINR, P5-7259, Dubna,1973.

16. Saethre Ø. et al. Nucl.Phys., 1973, A207, p.486.
17. Beuscher H. et al. Z.Physik, 1973, 263, p.201.
18. Sunyar A.W. et al. Phys.Lett., 1976, 62B, p.283.
19. Krumlinde J., Szymanski Z., Phys.Lett., 1971, 36B, p.157.
20. Beuscher H. et al. Ann.Rep., KFA-IKP 10/74, 81, Jülich, 1974.
21. Husar D. et al. Phys.Rev.Lett., 1976, 36, p.1291.
22. Flerov G.N., Karnaukhov V.A. C.Rendus du Congres Int. de Phys.Nucl., 1964, Paris, v. 1, p.373.
23. Kalinkin B.N., Petcov I.J. Acta Phys. Polon., 1964, 25, p.265.
24. Tarantin N.I. In: "Nuclear Chemistry" Nauka, Moscow, 1965, p.182; JINR, P7-10342, P7-10343, Dubna, 1976.
25. Grover J.R. and Gilat J. Phys.Rev., 1967, 157, p.p.802, 814.
26. Stephens F.S. Proc. Int. Conf. on Properties of Nuclear States, Montreal Univ. Press, Montreal, 1969, p.271.
27. Cabot C. et al. J.Physique, 1975, L36, p.289; Gauvin H. et al. Phys.Rev., 1974, C10, p.722.
28. Plasil F., Blann M.Phys.Rev., 1975, C11, p.508.
29. Trautmann W. et al.Phys.Rev.Lett., 1975, 35, p.1694.

Received by Publishing Department
on May 20, 1977.